ISSN 0023-1584, Kinetics and Catalysis, 2010, Vol. 51, No. 5, pp. 678–690. © Pleiades Publishing, Ltd., 2010.
Original Russian Text © L.G. Bruk, O.N. Temkin, A.S. Abdullaeva, E.A. Timashova, E.Yu. Bukina, K.Yu. Odintsov, I.V. Oshanina, 2010, published in Kinetika i Kataliz, 2010, Vol. 51, No. 5, pp. 702–714.

Coupled Processes in Carbon Monoxide Oxidation: Kinetics and Mechanism of CO Oxidation by Oxygen in PdX_2–Organic Solvent–Water Systems

L. G. Bruk, O. N. Temkin, A. S. Abdullaeva, E. A. Timashova, E. Yu. Bukina, K. Yu. Odintsov, and I. V. Oshanina

Moscow State Academy of Fine Chemical Technology, Moscow, 119571 Russia
e-mail: lgbruk@mail.ru

Received October 22, 2009

Abstract—PdX_2–organic solvent–water solutions, where X = halide (preferably bromide or iodide) and the organic solvent is 1,4-dioxane or tetrahydrofuran, are suggested as catalytic systems for CO oxidation. A number of coupled processes take place in these systems. The kinetics and mechanism of CO oxidation by oxygen in the PdI_2–LiI–1,4-dioxane–water system are reported. Cyclohexene hydrocarboxylation into cyclohexanecarboxylic acid can be carried out as part of the coupled process occurring in the $PdBr_2$–tetrahydrofuran–water system.

DOI: 10.1134/S0023158410050095

The term coupled reactions is conventionally used to mean two reactions coupled through chemical induction [1]. The essence of this phenomenon is that a reaction subject to kinetic or thermodynamic limitations occurs owing to the simultaneous occurrence of a reaction having no such limitations. The basics of coupled reactions theory were devised by W. Ostwald and N.A. Shilov at the end of the 19th century and at the beginning of the 20th century [2].

Ostwald and Shilov's theory, which was formulated long before the appearance of the modern theory of multiroute and chain processes, was intended for phenomenological description of the interdependence of reactions. We should really give credit to these scientists, who were able to understand one hundred years ago that the necessary conditions for chemical coupling are the existence of multiple reaction routes and of at least one common intermediate for the supposedly coupled reactions. Later, the phenomenon of coupling was reduced to the concept of chemical induction and was thus separated into a special area of chemical kinetics [1, 3, 4].

The existence of a common intermediate for coupled reactions is a necessary, but not sufficient, condition for thermodynamic coupling. M. Boudart demonstrated that thermodynamic coupling can take place only when there is kinetic coupling between consecutive reactions (steps) due to the formation of an intermediate X [5]:

$$\begin{gathered} A \rightleftharpoons X + P_1, \\ X \rightleftharpoons C. \end{gathered} \tag{I}$$

If the second step ($X \rightleftharpoons C$) is exoergonic (has positive chemical affinity) and decreases the current concentration of X well below the equilibrium X concentration in the first, endoergonic step ($A \rightleftharpoons X + P_1$), the chemical affinity of the first step as part of the coupled process (I) will be positive. In this case, the steps of process (I) are kinetically and thermodynamically coupled and the formation rates of the products P_1 and C are related by the stoichiometric equation $A = P_1 + C$ (the conversion of X into C stimulates the formation of P_1 from A).

Another case of consecutive thermodynamic coupling is

$$\begin{gathered} A + B \rightleftharpoons X + P_2, \\ X \longrightarrow C. \end{gathered} \tag{II}$$

If the reactant A does not turn spontaneously into the product C, but this product can be obtained from the intermediate X, then this intermediate should be obtained from A and a reactant B in the first step of reaction (II). The product formation reactions will then be kinetically and thermodynamically related by the stoichiometric equation $A + B = P_2 + C$.

The rates of parallel reactions having a common intermediate are kinetically interrelated, but there can be no thermodynamic coupling in this case. There is the erroneous opinion that it is the parallel reactions that ensure thermodynamic coupling [4]. However, the only correct view of the subject is that of Ostwald, Lehninger, and Boudart, who claimed that thermodynamic coupling appears only in the case of consecutive reactions having a common intermediate.

Thus, the kinetic coupling of steps having common intermediates is a characteristic feature of reactions proceeding via a complex mechanism.

An analysis of numerous coupled reactions allows one to determine the role of classical chemical induction in the variety of kinetically coupled processes [6]. The existence of kinetic coupling with chemical induction in a single-route process (reactions (I) and (II)) can lead to the thermodynamic coupling of the exoergonic and endoergonic steps and to the formation of a stoichiometrically coupled process having no thermodynamic limitations [6, 7].

In two-route and multiroute reactions, kinetic coupling cannot cause the thermodynamic coupling of the overall reactions proceeding via different routes, although, for chain mechanisms, there is chemical induction as a significant acceleration of the reactions in one of the routes due to the simultaneous occurrence of reactions via the other routes [6–8].

The following scheme is typical for two-route processes having a common intermediate formation step:

$$A + B \longrightarrow X \begin{cases} \longrightarrow P_1 \\ \xrightarrow{+C} P_2 + P_3. \end{cases} \qquad \text{(III)}$$

In this mechanism, the two routes are described by their own overall equations.

A classical example of coupled reactions with chemical induction is the case in which process (IV) does not take place without reaction (V) for thermodynamic of kinetic reasons. Process (IV) is formally a part of the coupled process (VI):

$$A + C \longrightarrow P_2, \qquad \text{(IV)}$$

$$A + B = P_1, \qquad \text{(V)}$$

$$A + B + C = P_2 + P_3. \qquad \text{(VI)}$$

Chemical coupling can speed up thermodynamically possible chain reactions [6–8]. For example, the coupling between the route including the chain initiation and termination steps and the route including chain propagation increases the rate of the latter. The chain initiation step maintains a high concentration of the intermediate involved as the catalyst in the chain propagation route. The stoichiometric equation of the chain propagation route must be thermodynamically allowable. Free radicals are the reactive intermediates responsible for kinetic coupling in radical chain processes. In catalytic chain reactions, kinetic coupling is due to the catalysts forming in situ from the initial reactants [8].

The deliberate formation of a target product synthesis process by combining separate steps, sequences of steps, and routes involving common intermediates based on information about likely mechanisms of these conversions will be called the kinetic coupling (KC) principle. Since the appearance of the classical works in alkene oxidation [9, 10], this principle has been used in the design of catalytic systems over more than 60 years. In particular, the polyfunctional catalytic systems PdX_2–CuX_2, PdX_2–heteropoly acid, PdX_2–quinone, and others ensure the consecutive coupling of stoichiometric alkene oxidations by Pd(II) into different products (aldehydes, ketones, ethers, esters, and glycols) with the oxidation of the reduced form of palladium into the initial palladium(II) compound by the cocatalyst, thus forming a palladium(II)-based catalytic cycle.

Obviously, use of the KC principle in the design of catalytic systems is limited by the amount and quality of information concerning the likely mechanisms of the reactions to be coupled.

The oxidation of CO into CO_2,

$$CO + 0.5O_2 = CO_2 \qquad \text{(VII)}$$

is among the base reactions that are most frequently used in practice, whether voluntarily or not. Reaction (VII) can be a source of various intermediates and catalysts [8].

Here, we report the way in which reaction (VII) occurs in new liquid-phase catalytic systems based on palladium complexes. These systems include an aqueous–organic mixed solvent and do not contain a cocatalyst. We will demonstrate the possibility of designing coupled processes based on reaction (VII) using the KC principle.

Liquid-phase homogeneous catalytic systems based on transition metal compounds for carbon monoxide oxidation with atmospheric oxygen have been known for a long time [11]. Because oxygen is an insufficiently effective oxidizer for the reduced forms of the catalyst in most systems, copper(II) and iron(III) compounds, heteropoly acids, nitrites, *para*-quinones, and others are generally used as cocatalysts along with a Group VIII metal compound. The function of such a cocatalyst is to reoxidize the reduced form of the Group VIII metal. The reduced form of the cocatalyst should be rapidly oxidizable by oxygen under given conditions.

At the same time, some oxidation-type processes involving carbon monoxide are known to occur in organic solvents without a cocatalyst. An example of such a process is the oxidative carbonylation of alkynes in a ketone or nitrile medium [7]. It is, therefore, interesting to study carbon monoxide oxidation in $PdHal_2$–organic solvent–water systems.

EXPERIMENTAL

Kinetic experiments were carried out in a temperature-controlled gas flow reactor under vigorous stirring of the gas and liquid phases. This vigorous stirring ensured that the reaction proceeded under kinetic control. The products of the conversion of the initial reactants and solvents were identified by the GC/MS method. The reacting solution and the gas phase were analyzed by gas chromatography.

Table 1. Solvent effects

Solvent	T, °C	Initial gas composition, vol %		$[H_2O]$, mol/l	r_{CO_2}, mol l^{-1} h^{-1}
		O_2	CO		
1,4-Dioxane	30	76.5	23.5	1.6	0.75
1,4-Dioxane	30	76.0	24.0	1.7	0.79
1,4-Dioxane	40	74.4	25.3	2.49	0.98
THF	30	77.0	23.0	0.57	0.85
THF	30	76.4	23.6	1.4	0.77
THF	40	76.4	23.6	1.46	1.16
Diethylene glycol	30	75.0	25.0	0.51	0.17
Ethylene glycol	30	74.8	25.2	0.56	0.008
Acetonitrile	40	75.0	25.0	1.28	0.02
Acetone	40	75.4	24.6	1.53	0.03
Hexane	40	76.1	23.9	0.74	–
Chloroform	40	75.0	25.0	1.45	0.04
Methanol	40	74.4	25.4	2.79	0.02
Acetic acid	40	75.1	24.9	4.62	0.02
Dichloromethane	40	76.3	23.7	1.47	0.02
DMF	40	75.5	24.5	1.37	0.03

Note: The reactions were conducted in a gas-open system at $[PdBr_2] = 0.01$ mol/l.

The gas phase was analyzed using a column 3 m in length and 3 mm in diameter packed with activated carbon AR-3 (0.25–0.5 mm fraction, oven temperature of 140°C, argon as the carrier gas, thermal-conductivity detector). Oxygen, nitrogen, and carbon monoxide were quantified separately using a column with the same dimensions packed with molecular sieve 13X (0.25–0.5 mm fraction, oven temperature of 40°C, argon as the carrier gas, thermal-conductivity detector).

The solvents and the water content of the reacting solution were analyzed using a column with the same dimensions packed with Polisorb-1 (0.25–0.5 mm fraction, oven temperature of 160°C, helium as the carrier gas, thermal-conductivity detector).

γ-Butyrolactone and cyclohexene were quantified using a column 3 m in length and 3 mm in diameter packed with Porapak Q (oven temperature of 230°C, helium as the carrier gas, thermal-conductivity detector). Cyclohexanecarboxylic acid was determined using a 3-m-long glass column packed with 10% PPMS-4/Polikhrom-1 (oven temperature of 160°C, helium as the carrier gas, flame ionization detector).

The peroxide concentration in the palladium bromide–based reacting solution was determined by iodometric titration, and the acid concentration was determined pH-metrically with an instrument calibrated against known amounts of acid added.

The CO and O_2 absorption and CO_2 formation rates were derived from the compositions of the initial gas and the gas leaving the reactor after the process had come to a quasi-steady state.

The liquid reaction mixture was sampled during the run, and the samples were chromatographed. The time dependences of product concentrations were plotted from chromatographic data. From the slopes of the steady-state portions of the corresponding curves, we derived the initial rates (r) of the formation (disappearance) of the products (reactants).

RESULTS AND DISCUSSION

Selecting a Solvent and a Palladium Precursor

The nature of the solvent is among the most significant and hardly predictable factors having an effect on the homogeneous catalytic process. We tested organic compounds of the following classes as solvents

Table 2. Influence of the nature of the initial palladium compound on the carbon dioxide formation rate, 30°C

Catalyst*	Initial gas composition, vol %		r_{CO_2}, mol l^{-1} h^{-1}
	O_2	CO	
$PdBr_2$	70.8	29.2	0.88
$PdCl_2$	68.0	32.0	0.08
PdI_2	67.8	32.2	0.19

* The catalyst concentration is 0.004 mol/l.

for carbon monoxide oxidation: cyclic ethers, glycols, ketones, nitriles, alkanes, alcohols, acids, chlorohydrocarbons, and amides. The results of these tests (Table 1) indicate that the most efficient solvents are cyclic ethers, namely, 1,4-dioxane and tetrahydrofuran (THF). The CO oxidation rate in diethylene glycol is one order of magnitude lower, and that in the other solvents is lower by another order of magnitude. In most cases, the very low reaction rate is due to the rapid reduction of the greater part of Pd(II) and the formation of Pd(0) phase (palladium black).

Among the palladium halides, the best catalyst component for CO oxidation is palladium bromide (Table 2). Palladium chloride turns rapidly into palladium black, and the iodide ligand markedly lowers the activity of the catalyst (Table 2). The system based on palladium iodide turned out to be the most convenient for investigating the CO kinetics.

Reaction Stoichiometry

The stoichiometry of the main reaction occurring in the $PdBr_2$–organic solvent (1,4-dioxane or THF) system is similar to that of the reaction

$$CO + O_2 + H_2O \longrightarrow CO_2 + H_2O_2 \qquad \text{(VIII)}$$

in terms of the carbon monoxide and oxygen conversion and CO_2 formation rates (Table 3). The formation of peroxides (hydrogen peroxide, palladium peroxide, and organic peroxides) in the reaction system was detected by iodometric titration (Table 3).

The water concentration usually passed through a minimum during the run, while the peroxide concentration passed through a maximum, which was not higher than 0.5 wt % (0.15 mol/l in terms of H_2O_2). The hydrogen peroxide selectivity in terms of absorbed oxygen (*S*) decreases during the run (Fig. 1). This is evidence that process (VIII), which formally couples CO oxidation into CO_2 and H_2O oxidation into H_2O_2, is accompanied by some oxidation reactions that involve oxygen, hydrogen peroxide, or their derivatives and yield water.

Solvent conversion products were identified in the reacting solution under conditions of the coupled process (VIII) by GC/MS using the NIST mass spectral library. 1,4-Dioxane turns into 1,4-dioxene and 2-hydroxy-1,4-dioxane:

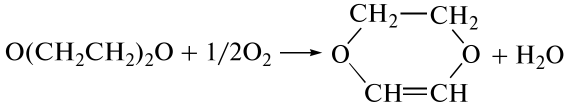

(IX)

Table 3. Data for determining the stoichiometry of the reactions occurring in $PdBr_2$–organic solvent systems

Solvent	$[H_2O]$, mol/l	Consumption or formation rate, mol l^{-1} h^{-1}			Amount of reacted or formed compound, mmol			$[H_2O_2]$, %
		O_2	CO	CO_2	O_2	CO	CO_2	
1,4-Dioxane	1.69	0.93	0.79	0.66	8.7	7.7	6.5	0.41
1,4-Dioxane	1.20	0.20	0.13	0.11	3.3	1.3	1.0	0.13
1,4-Dioxane	1.43	0.18	0.15	0.14	1.7	1.4	1.2	0.22
1,4-Dioxane	1.73	0.49	0.44	0.44	4.9	3.8	3.8	0.31
1,4-Dioxane	1.64	0.56	0.75	0.72	5.2	7.0	6.5	–
THF*	0.58	0.48	0.47	0.44	5.8	5.6	5.4	0.29
THF	0.88	~0.6	~0.6	~0.6	5.2	4.4	4.3	–
THF	0.54	0.4	0.45	0.35	2.2	4.3	2.8	0.32
THF**	0.54	0.5	0.7	0.7	5.2	7.6	6.6	0.16

Note: Reaction conditions: gas-open system, initial O_2/CO ratio of ~3.5, $[PdBr_2] = 0.01$ mol/l, $T = 30$°C, atmospheric pressure.
* $[PdBr_2] = 0.014$ mol/l.
** $[PdBr_2] = 0.011$ mol/l.

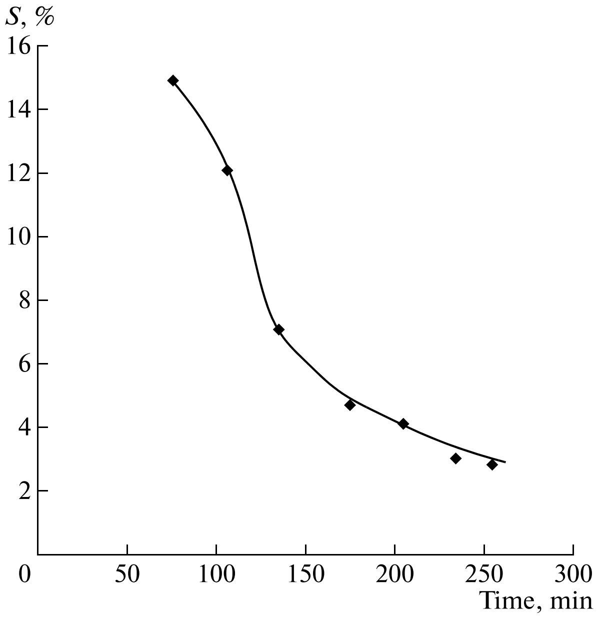

Fig. 1. H_2O_2 selectivity as a function of the reaction time.

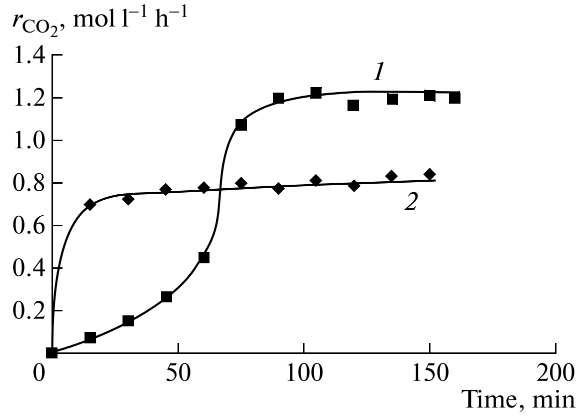

Fig. 2. Variation of the CO_2 formation rate during the reaction in 1,4-dioxane at 40°C: (*1*) $[PdBr_2] = 0.011$ mol/l; (*2*) $[Pd(CO)Br]_n = 0.01$ mol/l.

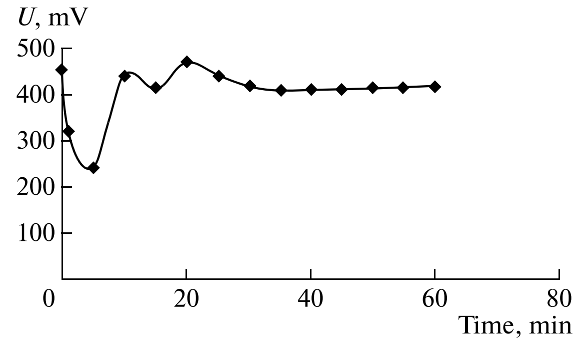

Fig. 3. Variation of the platinum electrode potential during the reaction. Reaction conditions: THF, 30°C, $[PdBr_2] = 0.01$ mol/l; $[H_2O] = 0.61$ mol/l; O_2 and CO partial pressures of 400 and 260 Torr, respectively.

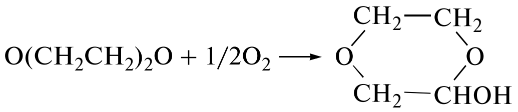
(X)

In addition, 1,4-dioxane conversion yields ethylene glycol monoformate and diformate:

$$O(CH_2CH_2)_2O + 2CO + 2H_2O \longrightarrow 2HOCH_2CH_2OOCH, \qquad (XI)$$

$$O(CH_2CH_2)_2O + 4CO + 2H_2O \longrightarrow 2HCOOCH_2CH_2OOCH. \qquad (XII)$$

γ-Butyrolactone and 1,4-dioxane were identified as THF conversion products:

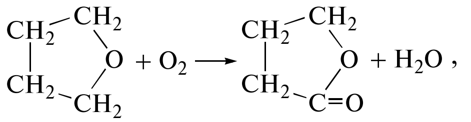
(XIII)

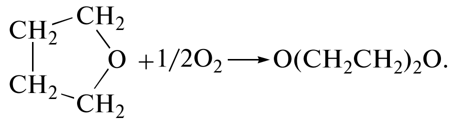
(XIV)

The mechanisms of reactions (IX)–(XIV) in this reaction system were not studied. Of particular interest are the mechanisms of 1,4-dioxane formation from THF and of formic acid formation from 1,4-dioxane and THF. Note that, at comparatively high palladium concentrations, both formaldehyde and formic acid are present in the reacting solution. It can, therefore, be assumed that formaldehyde results from reaction (XV), which is an example of the consecutive coupling of CO oxidation into CO_2 and CO reduction into formaldehyde:

$$2CO + H_2O \longrightarrow CO_2 + CH_2O. \qquad (XV)$$

It was demonstrated that this reaction can occur on dinuclear molybdenum complexes [12]. Formaldehyde oxidation by oxygen yields formic acid and its esters.

The oxygen balance will be satisfactorily satisfied if solvent oxidation yielding water via reactions (IX) and (XIII) is taken into account:

$$2\Delta n_{O_2} = \Delta n_{CO_2} + \Delta n_{H_2O},$$

where Δn_i is change in the number of moles of component *i* as a result of the process.

A period of development is observed for the process, during which the CO oxidation rate increases up to its steady-state value (Fig. 2, curve *1*). There is almost no development period when the palladium(I) complex $[Pd(CO)Br]_n$ synthesized as described by Kutyukov et al. [13] is used as the precursor (Fig. 2, curve *2*).

Measurements of the platinum electrode potential *U* (Fig. 3) and pH during the coupled process of CO oxidation into CO_2 and THF oxidation into γ-butyro-

Table 4. Effects of inhibitors (InH)

Solvent	[InH], mol/l	Initial gas, vol %		$[H_2O]$, mol/l	r_{CO_2}, mol l^{-1} h^{-1}	$[H_2O_2]$, %
		O_2	CO			
InH = ionol						
Dioxane	0.012	77.6	22.4	1.6	0.52	0.30
THF	0.011	76.5	23.5	0.65	0.55	0.25
InH = *para*-benzoquinone						
THF	0.008	76.3	23.7	0.54	0.88	–
THF	0.010	77.0	23.0	0.62	0.83	–
THF	0.10	76.2	23.8	0.59	0.74	–
Dioxane	0.10	76.9	23.1	1.7	0.72	–
Dioxane*	0.11	79.8	20.2	1.6	0.35	–
Dioxane	0.012	77.7	22.3	1.7	0.70	0.30
InH = hydroquinone						
Dioxane	0.010	77.8	22.2	1.7	0.44	0.31

Note: Reaction conditions: $[PdBr_2]$ = 0.01 mol/l, solution volume of 5 ml, T = 30°C.
* HBr (0.009 mol/l) was added to the reacting solution.

lactone suggested that, as the catalytic system forms, it first undergoes partial reduction (as is indicated by the minimum of U as a function of time) and then oxidizes to return into the initial state (U even exceeds the initial value). This is likely due to the appearance of palladium hydroperoxide. The pH of the solution changes from 3 to ~0 within 20 min and then remains practically invariable. According to our calibration, this pH value corresponds to an added acid concentration of 0.02 mol/l. This amount of acid might result from the complete hydrolysis of $PdBr_2$ in the system (0.01 mol/l) or from the complete reduction of palladium(II):

$$PdBr_2 + 2H_2O \longrightarrow Pd(OH)_2 + 2HBr, \qquad (XVI)$$

$$PdBr_2 + CO + H_2O \longrightarrow CO_2 + Pd(0) + 2HBr. \qquad (XVII)$$

The second variant is in conflict with the potentiometric data. Apparently, the main source of the acid is palladium halide hydrolysis, and minor sources are formic acid formation and solvent oxidation.

Thus, the results of our preliminary study can be summarized as follows.

The greater part of palladium during the process is in the oxidized form of Pd(II). An acid is present in the reacting solution in amounts comparable with the amount of palladium. This acid most likely results from the hydrolysis of the initial palladium(II) halide. The active catalyst forms via the reduction process Pd(II) ⟶ Pd(I).

The introduction of an inhibitor causes no significant changes in the CO_2 formation rate (Table 4). At this stage of our investigation, we did not gain information about the effect of inhibitors on the formation rates of the other products.

The above results suggest that, with 1,4-dioxane or THF as the solvent, several coupled reactions take place in the system. The base reaction is CO oxidation into CO_2, which accounts for approximately half the oxygen converted and yields an oxidizer (or oxidizers) stronger than dioxygen. This oxidizer can be hydrogen peroxide, palladium hydroperoxide, or organic hydroperoxides, and it involved in the oxidation of the solvent.

The following important questions arise when the mechanism of the coupled process (VIII) or similar processes occurring in CO oxidation into CO_2 is considered:

(1) What is the oxidation state of palladium in the catalytically active complexes?

(2) What form of the catalyst appears as a result of CO oxidation into CO_2?

(3) How is the catalytic cycle closed?

(4) in what way is dioxygen involved in this process? Does a palladium–dioxygen complex form? If so, what are its further conversions?

The above data suggest that, in the first approximation, the catalytic complexes are palladium(II) ones. The second question admits different answers. Zudin et al. [14], who carried out process (VIII) in the $PdCl_2$–PPh_3–CH_2Cl_2 system, suggested the following mechanism:

$$L_nPdX_2 + CO + H_2O \longrightarrow CO_2 + PdL_n + 2HX,$$
$$PdL_n + O_2 \rightleftharpoons L_nPd(O_2) \qquad \text{(XVIII)}$$
$$\xrightarrow{2HX} L_nPdX_2 + H_2O_2.$$

The key intermediate in this mechanism is the palladium(0) oxygen complex $L_nPd(O_2)$, which turns into hydrogen peroxide under the action of an acid. The triphenylphosphine ligand L stabilizes the palladium(0) complex. In the system examined here, the probability of the formation of a comparatively stable Pd(0) complex is much lower because of the absence of a phosphine ligand; however, palladium(0) compounds can be stabilized by the bromide ion or carbon monoxide. In addition, it is not impossible that the oxidation of carbon monoxide into carbon dioxide is catalyzed by a palladium(0) complex [15].

We think that the most likely mechanism is that involving the palladium hydrido complex:

$$PdX_2 + CO + H_2O \longrightarrow CO_2 + HPdX + HX,$$
$$HPdX + O_2 \longrightarrow HPdOOH \xrightarrow{HX} PdX_2 + H_2O_2. \qquad \text{(XIX)}$$

Indirect evidence in favor of the formation of the palladium hydrido complex is formaldehyde formation from carbon monoxide:

$$CO + HPdX + HX \longrightarrow CH_2O + PdX_2. \qquad \text{(XX)}$$

Since most of the hydrogen peroxide (or palladium hydroperoxide) is spent on the oxidation of the solvent, the following reaction should be taken into account when considering the stoichiometry of the process occurring in the THF medium:

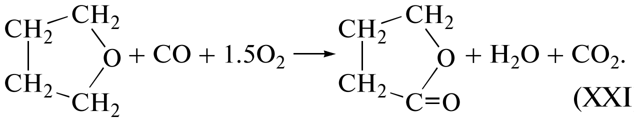

(XXI)

Hypotheses as to the Mechanism of CO Oxidation into CO_2 and Hydrogen Peroxide Formation

An analysis of the literature suggested two groups of hypotheses as to the mechanism of CO oxidation into CO_2.

In the first-group mechanisms, it is assumed that the only key intermediate in CO_2 formation is a palladium(II) or palladium(I) hydroxycarbonyl complex. This complex can form via several routes.

Route A is the replacement of anionic ligands in the palladium complex by carbon monoxide, water, and solvent molecules. An activated water molecule in the coordination sphere of palladium can undergo deprotonation. The hydroxycarbonyl complex results from intramolecular nucleophilic attack by the hydroxyl ligand on the carbon monoxide molecule activated in the coordination sphere of palladium:

$$PdX_4^{2-} + CO \rightleftharpoons PdX_3(CO)^- + X^-, \qquad \text{(XXII)}$$
$$PdX_3(CO)^- + H_2O \rightleftharpoons PdX_2(CO)(H_2O) + X^-,$$
$$PdX_2(CO)(H_2O) \overset{H_2O}{\rightleftharpoons} PdX_2(CO)(OH)^- + H_3O^+,$$
$$PdX_2(CO)(OH)^- + CO \rightleftharpoons PdX_2(CO)(COOH)^-.$$

When strong ligands are lacking, the coordination sphere of palladium can contain organic solvent molecules having a lone pair.

Route B includes nucleophilic attack by a water molecule from the outer sphere on the carbonyl ligand of palladium(II) or palladium(I):

$$PdX_4^{2-} + CO \rightleftharpoons PdX_3(CO)^- + X^-,$$
$$PdX_3(CO)^- + H_2O \rightleftharpoons PdX_3(COOH_2)^-, \qquad \text{(XXIII)}$$
$$PdX_3(CO)^- + H_2O \rightleftharpoons PdX_3(COOH)^{2-} + H^+.$$

Apparently, two palladium hydroxycarbonyl complexes can form here, one protonated and the other nonprotonated.

The decomposition of the hydroxycarbonyl complex with carbon dioxide formation most likely occurs as hydrogen β-elimination from the hydroxyl group, yielding a palladium hydrido complex. It is also possible that CO_2 formation involves the solvent, which can serve as a base to bind a proton:

$$PdX_2(CO)(COOH)^- \longrightarrow CO_2 + HPd(CO)X_2^-,$$
$$PdX_3(COOH_2)^- + :B$$
$$\longrightarrow HPdX_3^{2-} + BH^+ + CO_2, \qquad \text{(XXIV)}$$
$$PdX_3(COOH)^{2-} + :B + CO$$
$$\longrightarrow Pd(CO)X_3^{3-} + CO_2 + BH^+.$$

In the latter case, the decomposition of the palladium hydroxycarbonyl complex yields a Pd(0) compound stabilized by carbon monoxide and anions. It was demonstrated that Pd(0) compounds can be stabilized by anions [16], and the existence of Pd(0) carbonylhalo complexes has recently been proved experimentally [17]. However, it is likely that these compounds are likely unstable and decompose readily to yield palladium black.

The second group of CO_2 formation mechanisms is made up of those involving Pd(0) complexes that can result from the reduction of Pd(II) and Pd(I) com-

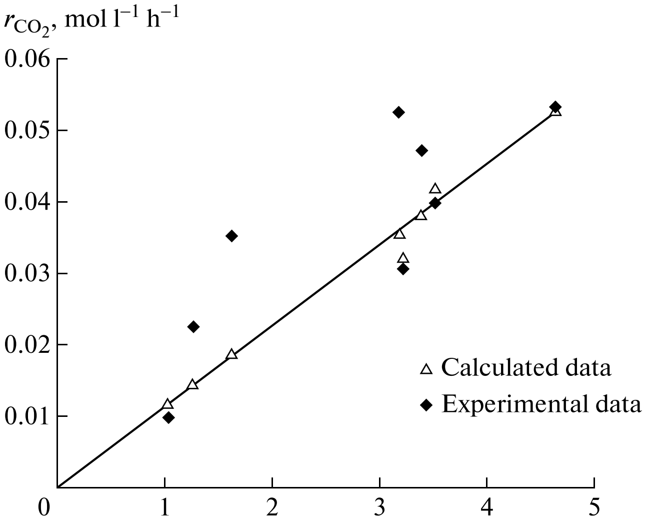

Fig. 4. CO_2 formation rate as a function of [H_2O]. Reaction conditions: 1,4-dioxane; 30°C; [PdI_2] = 0.006 mol/l; O_2 and CO partial pressures of 460 and 200 Torr, respectively. The line represents the data calculated using Eq. (6), and the points represent experimental data.

pounds in the oxidative conversions of carbon monoxide, ligands, and solvents (mechanism C):

$$Pd(II) + CO + H_2O \longrightarrow Pd(0) + CO_2 + 2H^+,$$

$$Pd(0) + O_2 \rightleftharpoons Pd(O_2),$$

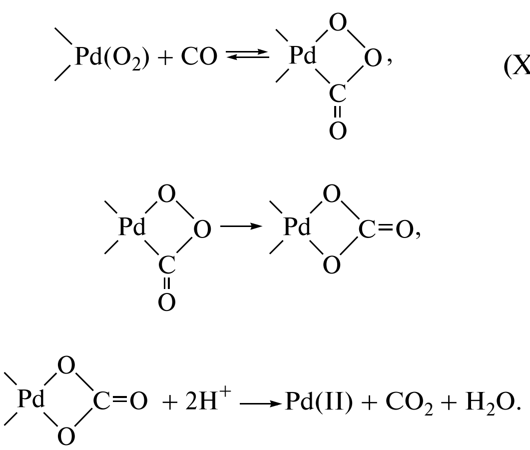

(XXV)

Mechanism C includes two sequences of reactions yielding carbon dioxide. The first includes Pd(II) reduction to Pd(0) and likely involves the palladium hydroxycarbonyl complex. The second includes the conversion of the Pd(0) oxygen complex via Pd(II) carbonate.

By analogy with the mechanism of coupled carbon monoxide and ethylene oxidation [18], the following mechanism can be suggested for carbon monoxide oxidation catalyzed by the Pd(0) complex forming from the Pd(II) compound introduced into the system:

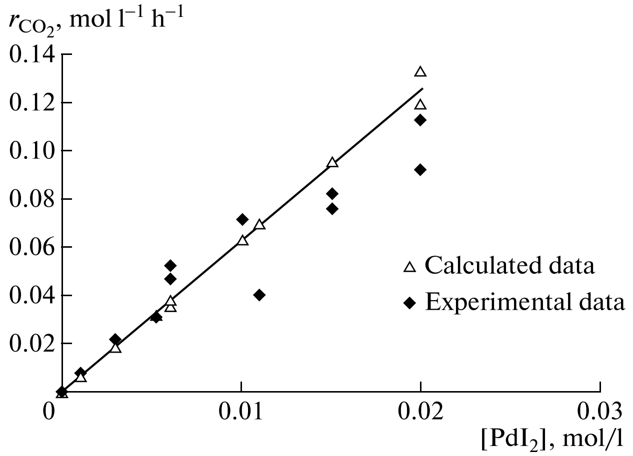

Fig. 5. CO_2 formation rate as a function of [PdI_2]. Reaction conditions: 1,4-dioxane; 30°C; [H_2O] = 3.4 mol/l; O_2 and CO partial pressures of 460 and 200 Torr, respectively. The line represents the data calculated using Eq. (6), and the points represent experimental data.

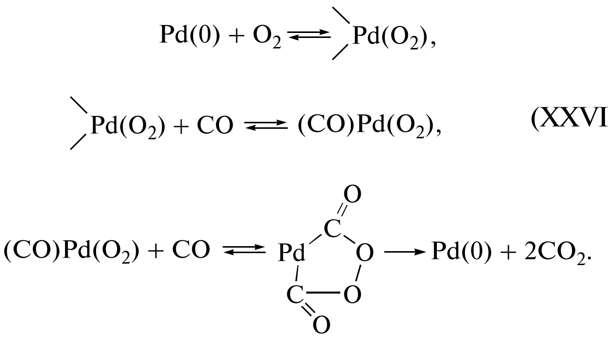

(XXVI)

Kinetics

In order to construct a complete kinetic model for CO oxidation into CO_2, we studied reaction kinetics in the PdI_2–LiI–H_2O–1,4-dioxane system for the reason that this system allows more reproducible results to be obtained than the $PdBr_2$–H_2O–1,4-dioxane system. These systems show nearly identical kinetic behaviors. Due to the comparatively low reaction rate in the iodide systems and due to the vigorous stirring of the phases, the process was kinetically controlled. The LiI concentration was 0.15 mol/l, and this ensured complete palladium iodide dissolution and the constancy of the palladium complexation function as all factors were varied. The carbon dioxide formation rate (r_{CO_2}) is a nearly linear function of [H_2O] up to a water concentration of 4 mol/l (Fig. 4). In the absence of water and at low water concentrations, the reaction does not take place, as in the case of the palladium bromide–based system. Therefore, in the first approximation, the mechanisms in which CO is oxidized by

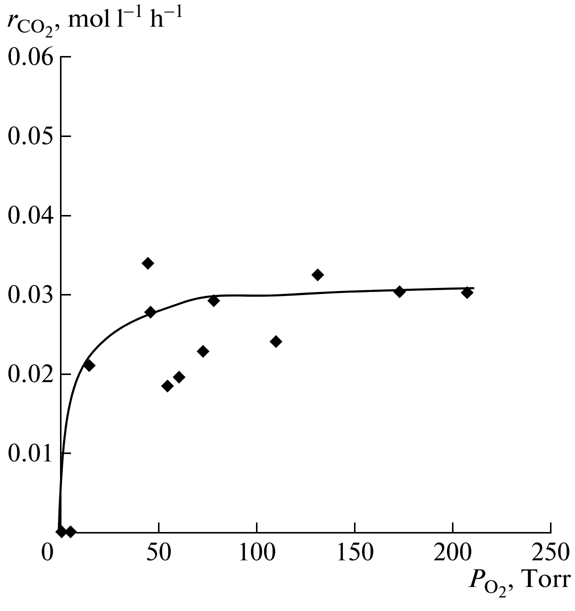

Fig. 6. CO_2 formation rate as a function of the O_2 partial pressure. Reaction conditions: 1,4-dioxane, 30°C, $[PdI_2]$ = 0.006 mol/l, $[H_2O]$ = 3.4 mol/l, P_{CO} = 230 Torr.

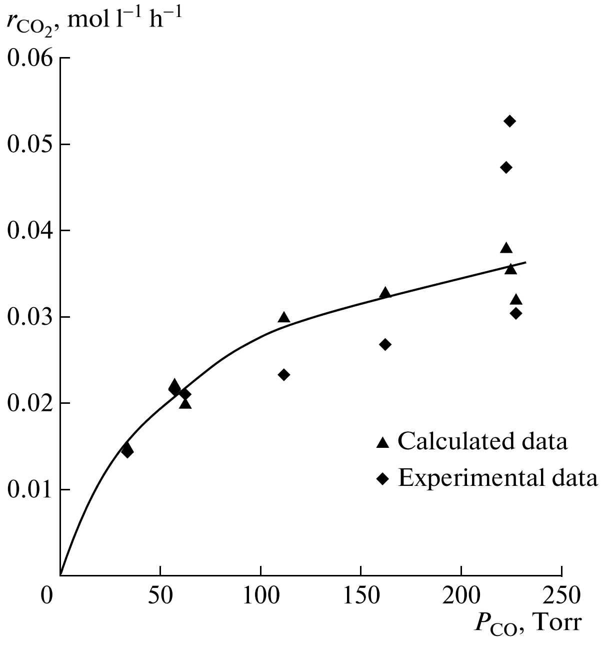

Fig. 7. CO_2 formation rate as a function of the CO partial pressure. Reaction conditions: 1,4-dioxane, 30°C, $[PdI_2]$ = 0.006 mol/l, $[H_2O]$ = 3.4 mol/l, P_{O_2} = 530 Torr. The line represents the data calculated using Eq. (6), and the points represent experimental data.

oxygen directly in the coordination sphere of palladium can be left out of consideration.

The dependence of r_{CO_2} on the palladium iodide concentration is satisfactorily described by a first-order equation throughout the concentration range examined (Fig. 5). The dependences of the CO_2 formation rate on the O_2 and CO partial pressures appear as curves tending to a limit (Figs. 6, 7, respectively). Starting at an O_2 concentration of 2 vol % in the feed gas, r_{CO_2} is practically independent of the oxygen partial pressure (Fig. 6).

The dependences of the CO_2 formation rate on the acid concentration in the iodide and bromide systems are similar. As the toluenesulfonic acid (TSA) concentration in the system is raised, r_{CO_2} falls sharply (Fig. 8). In the iodide system, the CO_2 formation rate after this sharp decrease comes to a constant level that does not vary as the acid concentration is further increased. The formal order of r_{CO_2} as a function of $[H^+]$ in the iodide system, determined from the $\log r_{CO_2}$ versus $\log[TSA]$ relationship, is approximately –0.5. The entire experimental data array (Fig. 9) can be satisfactorily fitted to the empirical equation

$$r_{CO_2} = k_{app}[Pd]_\Sigma[H_2O]P_{CO}/((1 + k'_{app}P_{CO})[H^+]) \quad (1)$$

with the apparent constants $k_{app} = 1.4 \times 10^{-2}$ h^{-1} Torr^{-1} and k'_{app} = 9.78 Torr^{-1}. The residual sum of squared deviations is 0.642×10^{-2}.

Discrimination of Hypotheses

Preliminary experiments and kinetic studies enabled us to discriminate hypotheses as to the mechanism of the process examined. Rate constants were estimated using a functional minimum search program based on the spiral descent method. The resulting relationships were compared with available experimental data. The most likely mechanism was determined by using the minimum residual sum of squared deviations as the criterion and by visually comparing the experimental data with the calculated product formation rates.

The near-zero order of the CO_2 formation reaction with respect to oxygen makes it possible to exclude the mechanisms in which direct CO oxidation by oxygen takes place, catalyzed by palladium(0) compounds (reaction (XXVI)). If this were the case, the order of the reaction with respect to oxygen would be higher, particularly at low O_2 partial pressures. The complex between Pd(0) and O_2 is unstable in the absence of strong stabilizing ligands.

A different situation takes place for the mechanisms that include two sequences of steps yielding carbon dioxide. If the rate-limiting step is Pd(II) reduction to Pd(0) (reaction (XXV)), the order of the reac-

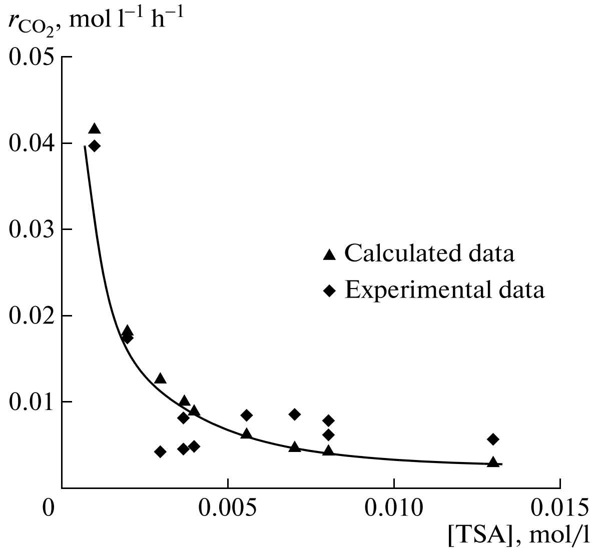

Fig. 8. CO_2 formation rate as a function of the toluenesulfonic acid concentration. Reaction conditions: 1,4-dioxane, 30°C, $[PdI_2] = 0.006$ mol/l, $[H_2O] = 3.5$ mol/l, $[LiI] = 0.15$ mol/l, $P_{O_2} = 430$ Torr, $P_{CO} = 230$ Torr. The line represents the data calculated using Eq. (6), and the points represent experimental data.

tion with respect to oxygen can be zero. Since the CO_2 formation rate is almost independent of the oxygen partial pressure down to very small P_{O_2} values, this CO_2 formation mechanism can hardly play a significant role in the process. The CO_2 formation rate changes very slightly as the oxygen partial pressure is decreased by a factor of 35 (Fig. 6). However, this mechanism cannot be excluded with certainty because of the rather wide scatter of the CO_2 formation rate versus oxygen partial pressure data points. Note that this scatter is due to the fact that the observed dependences are not strictly single-factor ones. As one factor is varied, the other factors inevitably change to some extent. In addition, "constant" factors somewhat change during the quasi-steady-state period, which is the time over which the reaction rate is measured.

Since there is no other information concerning the realization of the mechanisms that include direct carbon monoxide oxidation by oxygen in the system, we will discuss only mechanisms involving palladium hydroxycarbonyl complexes. These mechanisms include palladium halide hydrolysis steps, which yield OH groups coordinated to palladium. The detailed mechanism of ligand replacement is not considered within the mechanisms discussed here. Below, we will present several variants of the reaction mechanism involving a palladium hydroxycarbonyl complex, as well as the results of kinetic data processing in terms of the equations following from these mechanisms. All of the equations presented below contain apparent constants.

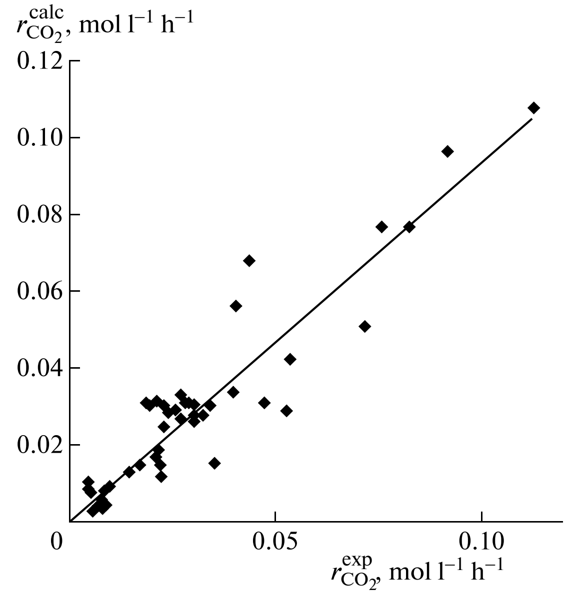

Fig. 9. Fit between calculated and experimental data for calculations r_{CO_2} using Eqs. (1) and (5).

In the first variant, there are two quasi-equilibrium palladium(II) iodide hydrolysis steps and a step of hydrogen β-elimination from the hydroxycarbonyl group:

$$\begin{gathered}\mathrm{S(CO)PdI_2 + H_2O \xrightleftharpoons{K_1} S(CO)PdI(OH) + HI,}\\ \mathrm{S(CO)PdI(OH) + H_2O}\\ \mathrm{\xrightleftharpoons{K_2} (CO)Pd(OH)_2 + HI,}\\ \mathrm{(CO)Pd(OH)_2 + CO}\\ \mathrm{\xrightleftharpoons[k_{-3}]{k_3} (CO)Pd(OH)(COOH),}\\ \mathrm{(CO)Pd(OH)(COOH)}\\ \mathrm{\xrightarrow{k_4} (CO)Pd(OH)(H) + CO_2.}\end{gathered} \qquad \text{(XXVII)}$$

Fitting the kinetic data to the equation

$$r_{CO_2} = k_1[Pd]_\Sigma[H_2O]^2P_{CO}/[H^+]^2, \qquad (2)$$

which was set up without palladium complexation taken into account, did not provide satisfactory results. This is obviously due to the fact that the orders of the equation with respect to the water and proton concentrations and carbon monoxide partial pressure are different (compare Eqs. (1) and (2)).

The other variant includes a single palladium iodide hydrolysis step:

$$\begin{gathered}\mathrm{S(CO)PdI_2 + H_2O \xrightleftharpoons{K_1} S(CO)PdI(OH) + HI,}\\ \mathrm{S(CO)PdI(OH) + CO}\\ \mathrm{\xrightleftharpoons{K_2} S(CO)PdI_2(COOH),}\\ \mathrm{S(CO)PdI_2(COOH) \xrightarrow{k_3} S(CO)PdIH + CO_2.}\end{gathered} \qquad \text{(XXVIII)}$$

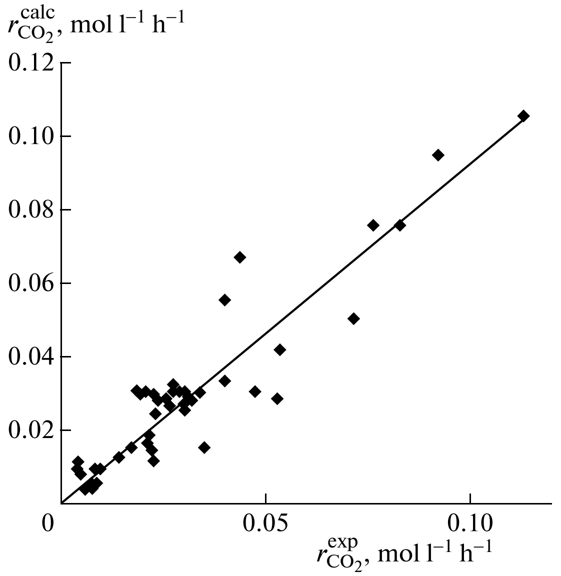

Fig. 10. Fit between calculated r_{CO_2} and experimental data for calculations using Eq. (6).

Fitting the kinetic data to the equation

$$r_{CO_2} = k_1[Pd]_\Sigma[H_2O]P_{CO}/[H^+], \qquad (3)$$

which was also obtained without palladium complexation taken into account, provided results only little better than were observed in the previous case. This is likely due to the incorrect order of the equation with respect to the carbon monoxide partial pressure.

If it is taken into account that the part of palladium coordinated in the S(CO)PdI(OH) intermediate is comparable with the total amount of palladium in the system, the following sum will appear in the denominator of the equation:

$$r_{CO_2} = k_1[Pd]_\Sigma[H_2O]P_{CO}/([H^+] + k_2[H_2O]), \qquad (4)$$

where k_1 = 0.2 h^{-1} Torr^{-1} and k_2 = 9.97. Here, the residual sum of squared deviations is 1.09 × 10^{-2}. However, Eq. (4) provides only a slightly better fit to experimental data than Eq. (3).

In the next variant of the mechanism, it is assumed that the quasi-equilibrium hydrolysis step is followed by an intramolecular nucleophilic attack of the hydroxyl group on the carbonyl group and that the vacated coordination site is occupied by a solvent molecule:

$$\begin{gathered}
S(CO)PdI_2 + H_2O \overset{K_1}{\rightleftharpoons} S(CO)PdI(OH) + HI,\\
S(CO)PdI(OH) + S \underset{k_{-2}}{\overset{k_2}{\rightleftharpoons}} S_2IPd(COOH),\\
S_2IPd(COOH) + CO \qquad\qquad (XXIX)\\
\underset{k_{-3}}{\overset{k_3}{\rightleftharpoons}} SIPd(CO)(COOH) + S,\\
SIPd(CO)(COOH) \xrightarrow{k_4} SIPd(H)(CO) + CO_2.
\end{gathered}$$

The equation following from this mechanism without palladium complexation taken into account,

$$r_{CO_2} = k_1[Pd]_\Sigma[H_2O]P_{CO}/([H^+](1 + k_2P_{CO})) \qquad (5)$$

is identical to the empirical equation (1) and provides a satisfactory fit to experimental data (Fig. 9).

With this mechanism, there is a conflict between the dependence of the reaction rate on the acid concentration according to Eq. (5) (which follows from mechanism (XXIX)) and the experimental dependence of r_{CO_2} on the acid concentration (Fig. 8). We attempted to eliminate this inconsistency by introducing mechanism (XXX), which includes the formation of the protonated and nonprotonated forms of the hydroxycarbonyl complex ($SPd(COOH_2)I_2$ and $SPd(COOH)I_2^-$, respectively, as a result of outer-sphere attack by water on coordinated CO:

$$\begin{gathered}
S_2PdI_2 + CO \overset{K_1}{\rightleftharpoons} SPd(CO)I_2 + S,\\
SPd(CO)I_2 + H_2O \overset{K_2}{\rightleftharpoons} SPd(COOH_2)I_2,\\
SPd(COOH_2)I_2 \overset{K_3}{\rightleftharpoons} SPd(COOH)I_2^- + H^+, \quad (XXX)\\
SPd(COOH_2)I_2 \xrightarrow{k_4} SPd(H)I_2^- + H^+ + CO_2,\\
SPd(COOH)I_2^- \xrightarrow{k_5} SPd(H)I_2^- + CO_2.
\end{gathered}$$

Either form undergoes β-elimination to yield palladium hydrido complexes.

Reaction mechanism (XXX), which takes into account palladium complexation in the intermediate $SPd(CO)I_2$, leads to Eq. (6). As compared to Eqs. (1) and (5), this equation provides an equally good fit to experimental data (see Fig. 10 and the partial dependences plotted in Figs. 5–8):

$$\begin{gathered}
r_{CO_2} = (k_1[Pd]_\Sigma[H_2O]P_{CO}(1\\
+ k_2[H^+]))/([H^+](1 + k_3P_{CO})),
\end{gathered} \qquad (6)$$

where k_1 = 2.3 × 10^{-5} h^{-1} Torr^{-1}, k_2 = 3.81 l mol^{-1}, and k_3 = 1 × 10^{-2} Torr^{-1}. The residual sum of squared deviations is 0.61 × 10^{-2}.

Processing of the kinetic data with the preliminary experiments taken into consideration demonstrated that the most likely carbon dioxide formation mechanisms are those involving palladium hydroxycarbonyl complexes (reactions (XXIX) and (XXX)). Our data provide no means to discriminate between the possible palladium hydroxycarbonyl formation mechanisms (inner-sphere versus outer-sphere nucleophilic attack on the coordinated carbonyl ligand).

We failed to obtain reliable kinetic data on the formation and disappearance of hydrogen peroxide and on the formation of dioxane conversion products, whose concentrations were too low for quantitative analysis to be carried out.

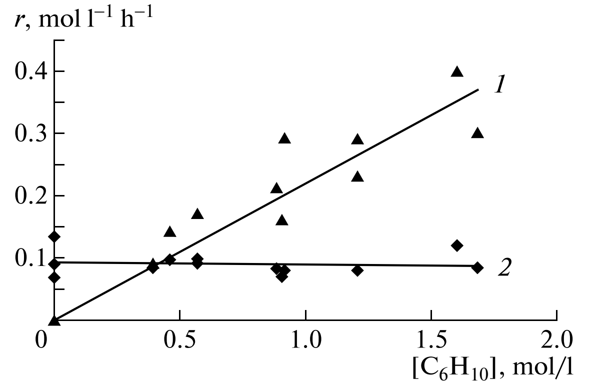

Fig. 11. (*1*) Cyclohexanecarboxylic acid and (*2*) γ-butyrolactone formation rates as a function of the initial cyclohexene concentration. Reaction conditions: THF, 30°C, $[PdBr_2] = 0.01$ mol/l, $[H_2O] = 0.5$ mol/l, $P_{O_2} = 460$ Torr, $P_{CO} = 200$ Torr.

It was established by special-purpose experiments that, when there is no carbon monoxide oxidation into carbon dioxide, hydrogen peroxide does not form and the solvent (1,4-dioxane or THF) does not oxidize. For example, when there is no palladium compound or CO in the reaction mixture, oxygen is not absorbed and no hydrogen peroxide or solvent oxidation products are detected in the solution. Therefore, the processes examined are coupled.

Coupled Process of Carbon Monoxide and THF Oxidation and Cyclohexene Hydrocarboxylation

The mechanism of palladium hydroxycarbonyl decomposition yielding palladium hydrido complexes was corroborated by experiments in which cyclohexene was introduced into the $PdBr_2$–THF–H_2O–CO–O_2 reaction system.

Along with the usual products of the coupled oxidation of CO, H_2O, and THF, cyclohexene conversion products were detected by chromatography and GC/MS at 30°C and atmospheric pressure (CO : O_2 = 30 : 70):

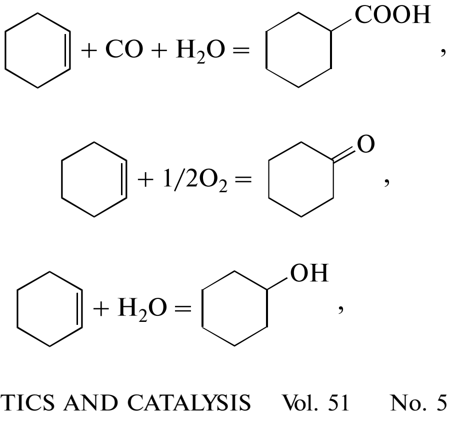

(XXXI)

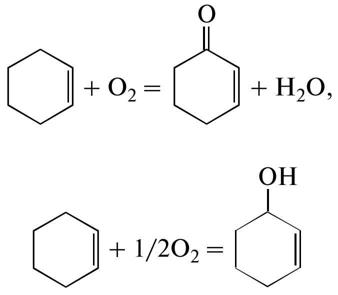

Cyclohexanecarboxylic acid and cyclohexanone form at the highest rates. In the absence of oxygen, cyclohexene carbonylation does not take place at 30°C and CO pressure of 1 atm. This proves that the oxidation and carbonylation processes are coupled.

The dependences of the cyclohexanecarboxylic acid and γ-butyrolactone formation rates on the cyclohexene concentration are plotted in Fig. 11. The former dependence is nearly linear, while the γ-butyrolactone formation rate remains almost unchanged as $[C_6H_{10}]$ is increased.

ACKNOWLEDGMENTS

This work was supported by the Russian Foundation for Basic Research (grant no. 08-03-00258).

REFERENCES

1. *Khimicheskaya entsiklopediya* (Encyclopedia of Chemistry), Moscow: Bol'shaya Rossiiskaya Entsiklopediya, 1995, vol. 4.
2. Shilov, N.A., *O sopryazhennykh reaktsiyakh okisleniya* (Coupled Oxidation Reactions), Moscow: Tipografiya Mamontova, 1905.
3. Nagiev, T.M., *Khimicheskoe sopryazhenie* (Chemical Coupling), Moscow: Nauka, 1989.
4. Nagiev, T.M., *Vzaimodeistvie sinkhronnykh reaktsii v khimii i biologii* (Coupling between Synchronous Reactions in Chemistry and Biology), Baku: Elm, 2001.
5. Boudart, M., *J. Phys. Chem.*, 1983, vol. 87, p. 2786.
6. Temkin, O.N., *Gomogennyi metallokompleksnyi kataliz: Kineticheskie aspekty* (Homogeneous Catalysis by Metal Complexes: Kinetic Aspects), Moscow: Akademkniga, 2008.
7. Bruk, L.G., Oshanina, I.V., Gorodskii, S.N., and Temkin, O.N., *Ros. Khim. Zh.*, 2006, vol. 50, no. 4, p. 103.
8. Bruk, L.G., Abdullaeva, A.S., Timashova, E.A., Bukina, E.U., Oshanina, I.V., and Temkin, O.N., *XVIII Int. Conf. on Chemical Reactors*, Malta, 2008, OP-I-7.
9. Smidt, J., Hafner, W., Jira, R., Sedlmeier, J., Sieber, R., and Sabel, A., *Angew. Chem.*, 1962, vol. 74, p. 93.

10. Moiseev, I.I., *π-Kompleksy v zhidkofaznom okislenii olefinov* (π-Complexes in Liquid-Phase Alkene Oxidation), Moscow: Nauka, 1970.
11. Rakitskaya, T.L., Ennan, A.A., and Paina, V.L., *Katalizatory nizkotemperaturnogo okisleniya monooksida ugleroda* (Catalysts for Low-Temperature Carbon Monoxide Oxidation), Moscow: TsINTIkhimneftemash, 1991.
12. Korol'kov, D.V. and Shchukarev, A.V., *Vestn. S.-Peterburg. Univ., Ser. 4: Fiz., Khim.*, 1992, no. 4, p. 34.
13. Kutyukov, G.G., Fasman, A.B., and Vozdvizhenskii, V.F., *Zh. Neorg. Khim.*, 1968, vol. 13, p. 1542.
14. Zudin, V.N., Likholobov, V.A., and Ermakov, Yu.I., *Kinet. Katal.*, 1977, vol. 18, no. 4, p. 921.
15. Kuznetsova, L.I., Matveev, K.I., and Zhizhina, E.G., *Kinet. Katal.,* 1985, vol. 26, no. 5, p. 1029.
16. Amatore, C. and Jutand, A., *J. Organomet. Chem.*, 1999, vol. 576, p. 254.
17. Kulik, A.V., Temkin, O.N., and Bruk, L.G., *Izv. Akad. Nauk, Ser. Khim.*, 2005, no. 6, p. 1349.
18. Zudin, V.N., Likholobov, V.A., and Ermakov, Yu.I., *Kinet. Katal.*, 1979, vol. 20, no. 3, p. 805.